Study of transverse domain wall dynamics in magnetic nanostrip of different shapes by using spin polarized current pulse

Madhurima Sen [1,2], *Koyel* Ganguly [1,2], *Saswati* Barman [1,2,*]

[1] Department of Basic Science and Humanities, Institute of Engineering & Management, Salt Lake Electronics Complex, Sector V, Salt Lake, Kolkata 700091, India

[2] University of Engineering & Management, University Area, Plot No. III, B/5, New Town Road, Action Area III, Newtown, Kolkata 700160, India

*Corresponding author email: saswati.barman@iem.edu.in

Abstract:

The controlled manipulation of domain walls in spintronic nanostructures is fundamental to advancing energy-efficient, high-speed memory and logic devices. In this study, we investigate the domain wall's dynamics in a magnetic nanostrip of continuously varying width and a magnetic nanostrip of uniform width under varying spin-polarized current densities. Domain walls are stabilized at distinct positions. Our findings reveal a strong dependence of domain wall mobility on both its initial stabilized position, the applied current, and the structure of the nanostrip. Notably, the domain wall's direction and the magnitude of the velocity of the domain wall are governed by an interplay between these factors, highlighting the complexity of domain wall dynamics driven by current. The present study reveals that it is possible to manipulate the domain wall velocity by varying the shape of the magnetic nanostrip. In a magnetic nanostrip with varying width, an additional potential barrier is generated, and the velocity and the pinning of the domain wall can be controlled. These insights provide a deeper understanding of domain wall motion driven by spin transfer torque, offering crucial implications for the next-generation spintronic architectures with enhanced control over domain wall transport for non-volatile memory and logic applications.

Keywords: Magnetic Domain wall, Transverse domain wall, Domain wall dynamics.

Introduction:

The potential use of magnetic domain wall movement in nanostructures for the creation of sophisticated spintronic devices has garnered a lot of interest, particularly magnetic memory devices [1], shift registers [2], and spin logic devices [3]. The racetrack memory introduced by Parkin *et al.* shows that magnetic domains can be used for storing information and domain walls can move when it subjected to pulse spin-polarized current [1]. On the other hand, Omari *et al.* suggest the use of magnetic domain walls to store the digital data instead of the magnetic domains [4]. Regardless of the various storage techniques of digital data, precise control over the domain wall manipulation is essential for implementing all these methods. Furthermore, the selective pinning of the domain wall at various positions is another crucial thing that has to be taken care of. So, a lot of intensive studies are performed by researchers on the domain wall dynamics in the magnetic wires and nanostrips by applying the magnetic field [5], and current [6]. Furthermore, various studies show the strain-driven magnetic domain wall motion [7] and domain wall motion by the thermal magnon current generated from the thermal gradients [8], and many more.

Spin transfer torque is produced when a ferromagnetic nanostrip is subject to a spin-polarized current, due to the spin angular momentum transfer from the itinerant electron to the local magnetization, resulting in the domain wall movement. The transverse domain wall aligns with the easy axis and propagates along the nanostrip's long axis when subjected to a spin-polarized current. Berger *et al*. predicted that the spin transfer torques have adiabatic contributions along with non-adiabatic contributions [9][10]. Apart from the adiabatic and non-adiabatic contributions, there are several physical mechanisms that exist that are crucial for understanding the domain wall dynamics, like linear momentum transfer, spin-flip scattering, etc. During the propagation of the domain wall, it dissipates energy due to Gilbert damping. The efficient control of the domain wall is a promising task that can be performed by introducing geometrical constrictions [11][12] and thickness inhomogeneities [13]. That constriction creates the potential for the local pinning in the domain wall, and that has to be overcome by the domain wall to move forward. That pinning potential can be created using structural engineering or geometric tailoring in various ways: notches [14], topological defects, and by changing the shape anisotropy. Yuan *et al.* studied the domain wall pinning at a notch when an external field is applied to it. It obtains the depinning field and provides the reason for the different depinning fields for the transverse domain wall having different chirality [15]. Hwang *et al.* investigate the effect of the boundaries and point defects on the domain wall dynamics [16]. In another study, the effect of the controlled artificial defects was studied, and the defect was induced by the patterning of the 1D domain wall dynamics on magnetic wires that are patterned in 2D ultrathin Co films [17]. Goolaup *et al.* proposed topological defects of the transverse domain wall for the deterministic pinning and movement of the domain wall within the complex network of conduits for the domain wall logic applications [18].

Apart from that, as Wiele *et al.* reported that the effect of the disorder on the domain wall dynamics on the permalloy nanostrip with a thin and narrow shape when it is subjected to the field or current. This study shows the two different pinning mechanisms at different regimes of the domain wall propagation [19]. Whereas, our study shows how the domain wall pinning can depend on the shape of the nanostrip and the initial position of the domain wall created in the stripe.

Therefore, the ability to precisely regulate the magnetic domain walls has unlocked new possibilities for developing more efficient, faster, and high-density data storage systems. This interesting field of research has a fundamental perspective along with some technical applications. This emerging technology holds the promise to change the computing landscape by enabling low-power logic devices and high-performance memory solutions. In this study, we are trying to observe the effect of the shape of the nanostrip on the domain wall dynamics subjected to spin-polarized current pulses with varying current density. Particularly, this study reveals the domain wall's velocity dependence, the domain wall's direction, and pinning and depinning of the domain wall on the different spin-polarized current densities and the various initial stabilized positions of the domain wall in magnetic nanostrips of constant width and continuously varying width.

Micromagnetic Simulation Details:

In this section, we have described the micromagnetic simulation process. In this study, we perform micromagnetic simulations to observe the difference between the domain wall dynamics in the nanostrip with continuously varying width (nanostrip - A) and the nanostrip with constant width (nanostrip - B). The domain wall dynamics in both the nanostrips are simulated through the micromagnetic simulation software named Object Oriented Micromagnetic Framework (OOMMF) [20]. The essential parameters for nanostrip-A, shown in Figure 1, are: material – permalloy, Length L = 5000 nm, thickness 8 nm, and varied width from 128.8 nm to 160 nm. The same parameters are used for nanostrip-B, except that it has a uniform width of 160 nm, and the schematics of the same are shown in Figure 2. Both the nanostrips are discretized with a cell size of 4 nm × 4 nm × 8 nm, where each side of the cell is smaller than the permalloy's exchange length. The simulation process is carried out in two phases: static simulation and dynamic simulation. The intention behind performing the static simulation is to stabilize the domain wall in the mentioned nanostrips. To obtain the static configuration, a square pulse of the magnetic field is applied with a magnitude of 10 Oe with a rise time, pulse width, and fall time of 1 ps each. The magnetic nanostrip attains the energy-minimized state or equilibrium within 20.04 ns and forms a transverse domain wall. We have used the value of the damping parameter α as 0.95 for getting the energy-minimized state quickly. In the static simulation, domain walls are formed at various positions. Following the static simulation, the dynamic simulation is conducted using the static domain wall configuration, and the dynamics of the domain wall are examined. To obtain the minimum energy state, the Landau-Lifshitz-Gilbert equation is solved. The time-dependent magnetization dynamics subjected to the applied spin-polarized current is studied by solving the modified Landau-Lifshitz-Gilbert equation as expressed by equation (1).

$$\frac{\partial \vec{m}}{\partial t} = \gamma\mu_0 \vec{H} \times \vec{m} + \alpha\, \vec{m} \times \left(\frac{\partial \vec{m}}{\partial t}\right) - (\vec{u}\cdot \vec{\nabla})\vec{m} + \beta\, [\vec{m} \times ((\vec{u}\cdot\vec{\nabla})\vec{m}] \quad (1)$$

where $\vec{H}$ is the micromagnetic effective field, and the gyromagnetic ratio is $\gamma = \boldsymbol{g}|\mu_B|/\hbar$. α is the Gilbert damping constant and $\vec{u}$ is the spin-drift velocity. The spin drift velocity is the velocity directed along the electrons' motion that is defined by the equation (2). It is the highest domain wall velocity that can be attained when the spin moments of the conduction electron are completely converted into the domain wall displacement. The spin drift velocity is given by:

$$u = \frac{jpg\mu_B}{2eM_S} \quad (2)$$

Where μ_B is the Bohr Magneton, g is Lande-g factor, M_S is the saturation magnetization, j is the current density, and P is spin polarization. For permalloy, $\vec{u} = \vec{J} \times \vec{P} \times 7\times 10^{-11}$ m^3/C [21]. The exchange interaction between the local magnetization and the direction of the spin polarization of the conduction electron causes the transfer of the momentum from the electron to the local magnetization, and the domain wall starts moving.

We have used α = 0.005 while obtaining the time-dependent magnetization data. Notwithstanding, the damping parameter of the permalloy is 0.008, but damping can change through doping, ion irradiation, and annealing. The value of spin polarization $\vec{P}$ is 0.4 during the entire simulation.

 https://doi.org/10.1051/epjconf/202532501014

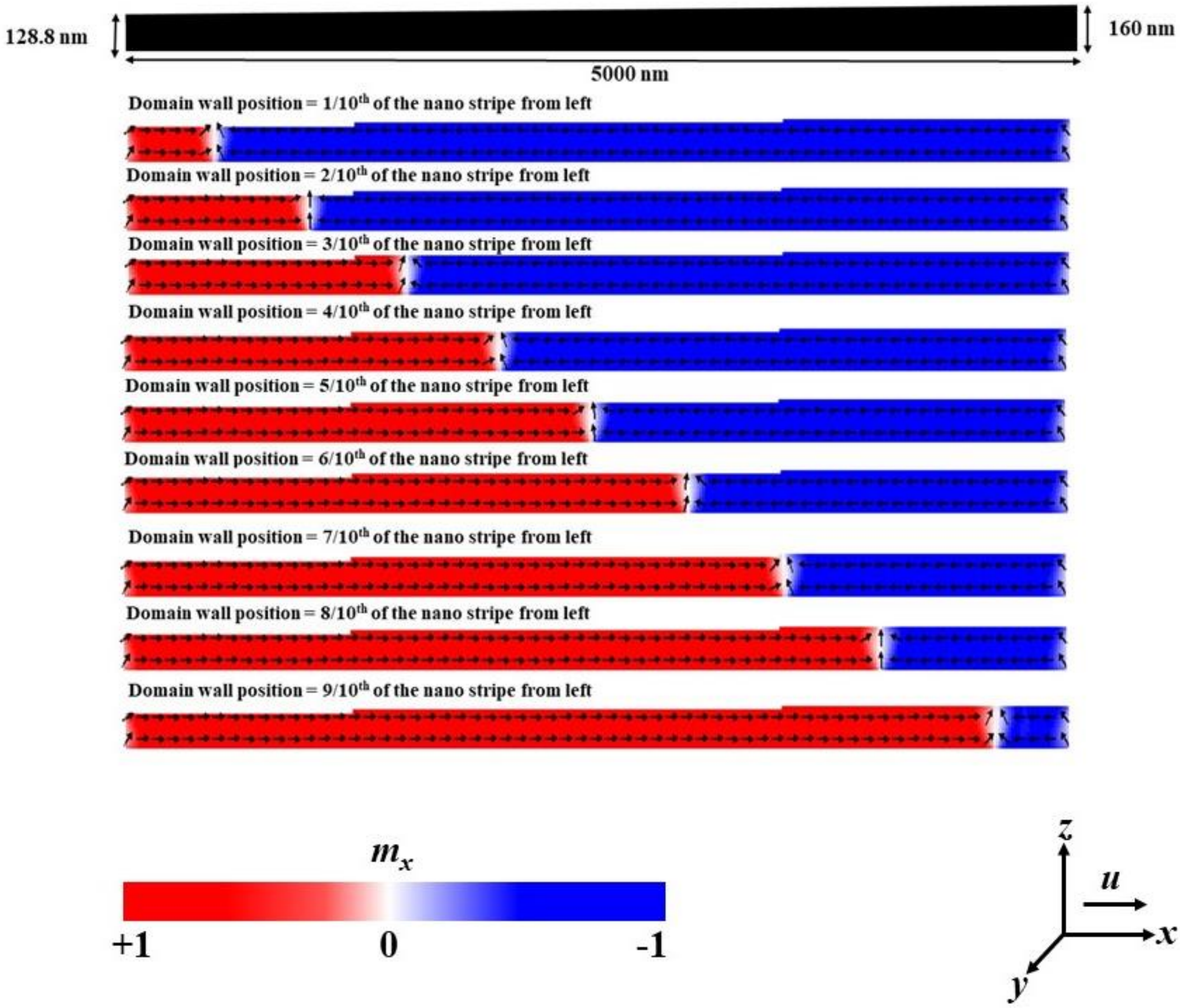

Figure 1: The domain wall's configuration after the static simulation at various positions in the nano stripe of continuously varying width (Nanostrip – A)

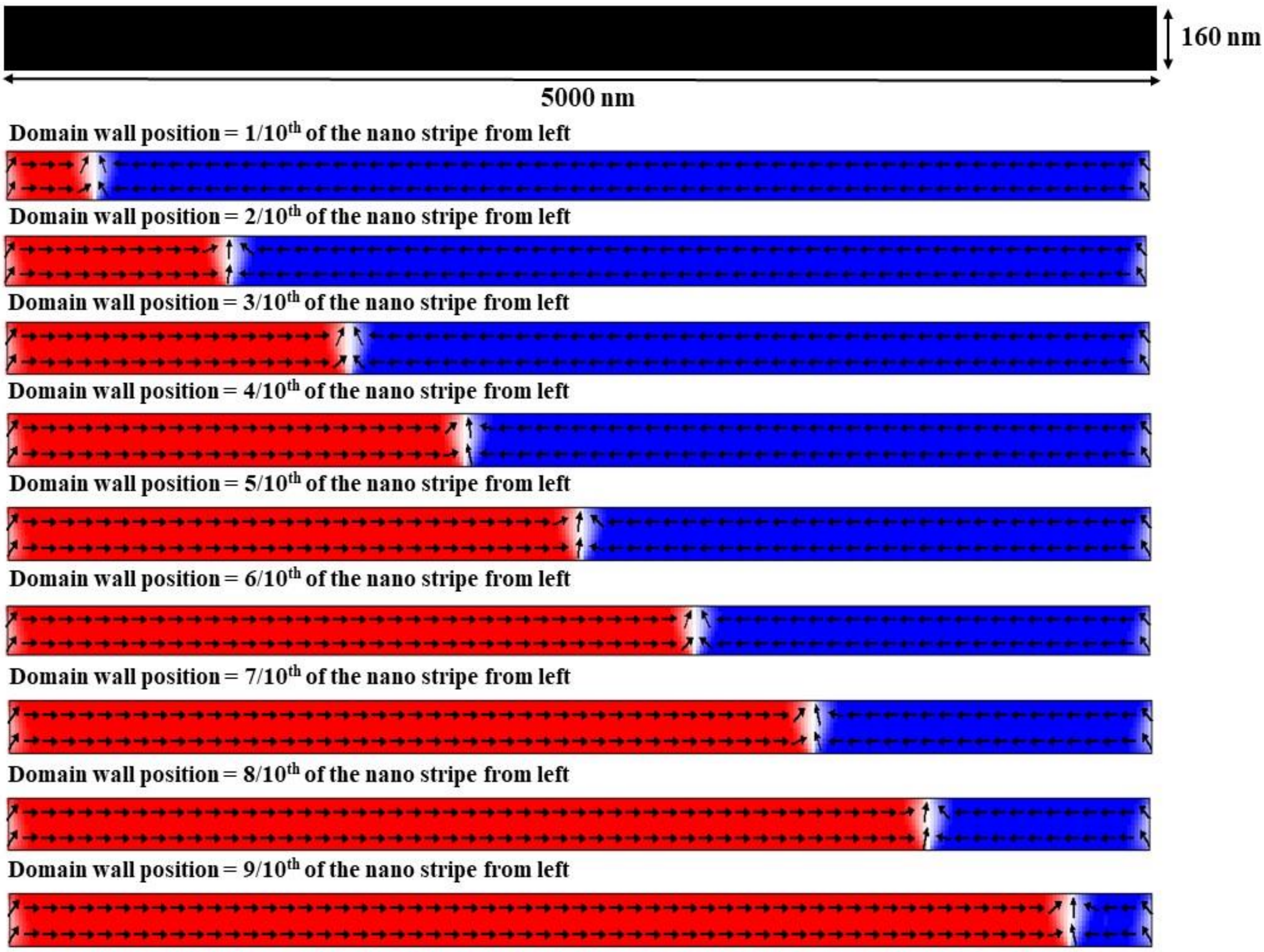

Figure 2: The domain wall's configuration after the static simulation at various positions in a simple straight nanostrip with constant width (Nanostrip – B).

The material parameters of the permalloy used in the simulation are mentioned in tabular form in Table 1. To obtain the time domain dynamics, we run the simulations for 20 ns.

Exchange constant	13 pJ/m
Saturation magnetization	800 kA/m
Magnetocrystalline anisotropy	0
Gilbert damping (α)	0.005
Non-adiabatic parameter (β)	0.05
Exchange length	5.3 nm

Table 1: Material parameters of the permalloy

The micromagnetic simulation determines the behavior of the domain wall when it is subjected to a sinc pulse spin-polarized current with spin drift velocity of u = 1 m/s, 5 m/s, and 40 m/s, representing the corresponding current densities J = 3.57×10^{10} A/m^2, 1.785×10^{11} A/m^2, and 1.42×10^{12} A/m^2, respectively.

The sinc pulse can be expressed as:

$$sinc\ (t)\ = \frac{\sin t}{t} \tag{3}$$

where $t = (total\ simulation\ time - pulse\ offset) \times pulse\ scale$

$$Pulse\ scale = \frac{2\pi}{Pulse\ period} \tag{4}$$

The pulse scale with the modification can be defined as

$$Pulse\ scale = k \times \frac{2\pi}{Pulse\ period} \tag{5}$$

The sinc pulse follows the sinc function defined in Equation 3. The variable t can be defined in terms of total simulation time, i.e., 20 ns, pulse offset, which is 0.05 ns, i.e., waveform displacement, and pulse scale, i.e., scaling factor. The pulse scale has been defined in equation 4. Pulse scaling has been done by using a scaler factor k that helps to increase the velocity of the domain wall significantly, as expressed in equation 5 [22]. In this simulation, k is 0.1 and the pulse period of the sinc pulse is 5 ns.

Results and Discussions:

To study the behaviour of the magnetic domain wall in a nanostrip - A and nanostrip - B, the domain wall was initially pinned at different positions within the strip. We define the domain wall's initial position as a distance from the left edge of the nanostrip. In this regard, a fraction of the total length of the nanostrip is considered. We have considered the domain wall's distance from the left edge of the nanostrip as L/10, 2L/10, 3L/10,…….., and 9L/10, where L represents the total length of the nanostrip. The dynamic behaviour of the domain wall depends upon the domain wall's position and the structure of the nanostrip. For understanding the domain wall dynamics, we have used spin-polarised current with current density ranging between 10^{10} and 10^{12} A/m².

Interestingly, this study shows that the displacement of the domain wall is not always possible by the exerted torque from the itinerant electron to local magnetization, when it is subjected to spin-polarized current. Primarily, the domain wall's movement varies depending on the initial position of the domain wall. We have presented the domain wall initially pinned at L/10 in nanostrip-A in Figure 3. When the spin polarized current is applied with u = 1 m/s, i.e., the current density 3.57 $\times 10^{10}$ A/m^2, the domain wall initially pinned at L/10 of the nanostrip-A does not get any momentum. A higher depinning current would be required to move the domain wall. As the initial pinning position of the domain wall shifts from the left edge towards the centre of the nanostrip, we observe an improvement in momentum transfer from the conduction electrons. For the initial pinning position of 2L/10 and 3L/10 in this nanostrip, the domain wall moves towards the left edge, i.e., in a direction opposite to the spin-polarized current's direction.

On the other hand, the domain walls in nanostrip – B, with initial pinning positions L/10/ 2L/10, 3L/10 moves toward the left of the nanostrip with a velocity of 329.3 m/s, 171.7 m/s and 96.7 m/s respectively signifying that the velocity of the domain wall decreases as the distance of its initial pinning position increase from the left age of the nano stripe. This is due to the fact that the domain wall formed at a considerable distance from the left edge experiences some potential barrier and a significant amount of energy is spent to cross the potential barrier, resulting in to slower domain wall velocity. However, in a nanostrip-A, the energy barrier in the positions 2L/10 and 3L/10 is lower since the domain walls are initially pinned near the tapered side of the nano stripe, resulting in higher domain wall velocities as compared to the domain walls formed at similar positions in a nanostrip B. As we move away from the left edge of the nano stripe, i.e., the initial pinning position of the domain wall is at 4L/10 in both the nano stripe, the domain walls show movement towards the left edge, and they get pinned after some time. Additionally, the domain wall in the nanostrip-A shows an oscillatory behaviour before getting pinned.

Nanostrip - A with the domain wall stabilized position of 5/10th, 6/10th, 7/10th, and 8/10th shows no movement for u =1 m/s, suggesting that it is unable to overcome the existing barrier potential at those positions. In contrast, the domain wall in nanostrip-B stabilized at 5L/10, 6L/10 positions move right and gets pinned after some time. For positions 7L/10, 8L/10, and 9L/10, the domain wall moves toward the right and completely passes the nanostrip-B with the higher velocities, 120 m/s, 196.4 m/s, and 358.5 m/s, respectively. Also, for nanostrip-A, the domain wall velocity is 195 m/s for the domain wall's initial position at 9L/10. These results signify the existence of an alternating barrier potential in nanostrip-A. On the other hand, the domain wall experiences lower barrier potentials nearer the edge of the nanostrips and significantly higher barrier potentials at the centre of the straight nano stripe.

When a slightly higher current with the spin drift velocity u = 5 m/s and the current density 1.785 $\times 10^{11}$ A/m^2 is applied in the nanostrip-A**,** a similar behavior is observed with some lower domain wall velocity as compared to u = 1 m/s for all the initial domain wall positions except at 9L/10. For the domain wall located at 9L/10, the domain wall moves at a velocity which is 1.5 times the velocity obtained with u = 1 m/s. For this current density, the general behavior of the domain wall and the direction of motion of the domain wall remains similar as compared to u = 1 m/s. However, the magnitude of domain wall velocity increases as the spin drift velocity u increases for the domain wall located between 3L/10 and 9L/10.

At u = 40 m/s with the current density 1.42 $\times$ 10^{12} A/m^2, it shows completely different micromagnetic dynamics, which is quite expected as a higher current is applied to it. Nearer the left end of the nanostrip - A, the domain wall moves to the right, oscillates, and gets pinned except for the domain wall at L/10, i.e., the wall located very close to the left end. The walls located near the right end of the stripe move with significant velocity towards the right and get pinned. On the other hand, the domain walls located between 5L/10 and 7L/10 show no movement at all. For a nanostrip-B, the domain walls located at all positions move with velocities ranging between 250 – 450 m/s. Existing literature on the current-driven domain wall dynamics reports domain wall velocities in the range 110 m/s – 400 m/s for current densities of the order of 10^{12} A/m^2. Miron *et al.* reported that the domain wall can attain a velocity of 400 m/s at a current density of 3.3 $\times$ 10^{12} A/m^2 in SIA structure of Pt(3nm)/Co(0.6 nm)/AlOx(2nm) [23]. In another study, Hayashi *et al.* attained the domain wall velocity of 110 m/s at the current density of 1.5$\times 10^8$ A/cm^2 in permalloy nanowires [24].

In general, the domain walls located near the right end of the nano stripe - A move with a slower velocity as compared to the nanostrip-B due to a higher potential barrier in nanostrip - A. The graphical representation of the domain wall velocity along with the initial position of the domain wall for the nanostrip-A and nanostrip-B is shown in Figure 3. In Figure 3, it has been shown the changes in the domain wall velocity with respect to the change in shape of the nanostrip. The data show that the no movement condition occurs for domain walls located between 5L/10 and 7L/10 for the nanostrip A for all the current densities. However, in the nanostrip-B, the domain walls do not move when they are located between 4L/10 and 5L/10 and at 3L/10 for the current densities 3.57 $\times 10^{10}$ A/m^2 and 1.785 $\times 10^{11}$ A/m^2, respectively. No movement condition does not occur for the nanostrip-B with a higher current density of 1.42 $\times 10^{12}$ A/m^2. However, the domain wall velocity drops in nanostrip-B with this higher current density when it is located at 4L/10.

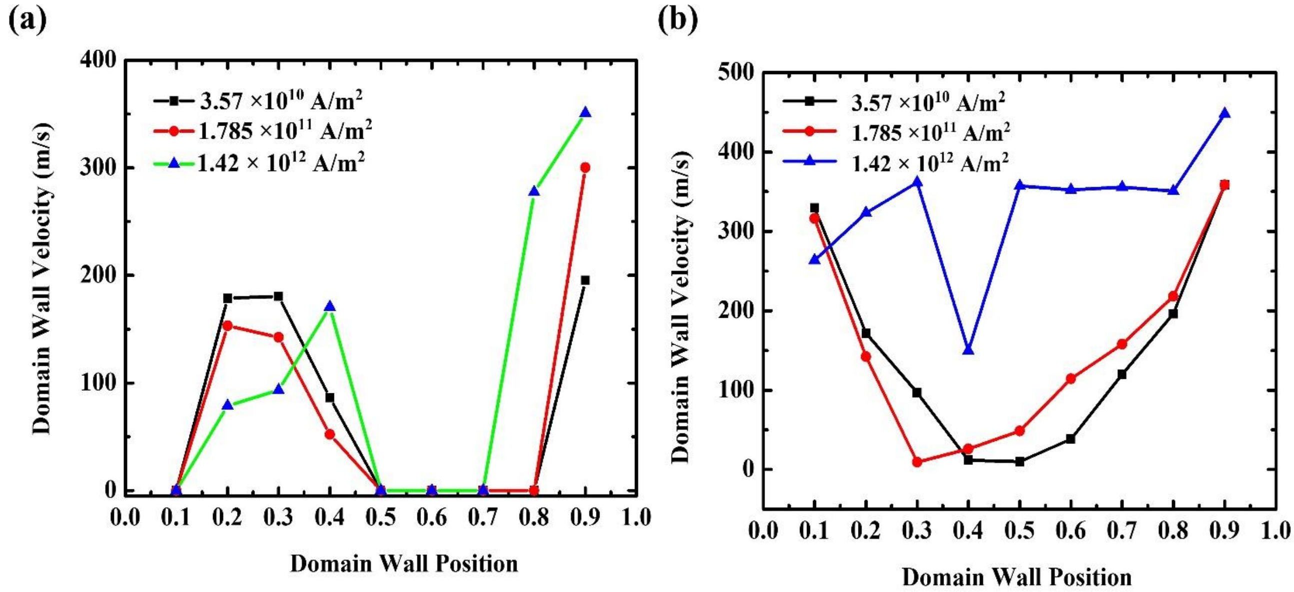

Figure 3: Position of the domain wall creation vs. domain wall velocity at three various current densities for the (a) nanostrip-A and (b) nanostrip-B.

Conclusions:

Our investigation into domain wall dynamics in a nanostrip with varying width and uniform width under varying spin-polarized current densities highlights the critical role of the initial stabilized positions and current-driven effects in determining domain wall velocity. Moreover, this new study shows the dependence of the direction of motion and the domain wall velocity on various factors. The findings demonstrate that the domain wall velocity varies significantly across different initial stabilized positions, with certain cases exhibiting negligible movement for the nanostrip-A. The domain wall velocity is dependent upon the shape of the nanostrip. In a nanostrip with continuously varying width, an additional potential barrier exists and limits the velocity of the domain wall to a completely pinned domain wall near the middle of the stripe. This study shows insights into having a firm hold on the control of the dynamics of the domain wall for the development of memory and logic devices. These insights contribute to the broader advancement of spintronic technologies, particularly in the development of energy-efficient and high-speed domain-wall-based memory and logic devices. Understanding these dynamics paves the way for improved control over domain wall motion, a crucial step toward the realization of next-generation spintronic applications.

References:

1. Parkin, M. Hayashi, and L. Thomas, Magnetic domain-wall racetrack memory. *science*, *320*(5873), pp.190-194 (2008).
2. Hayashi, L. Thomas, R. Moriya, C. Rettner, & S. S. P. Parkin, Current controlled magnetic domain wall nanowire Shift register. Science 320, 209 (2008).
3. D. A. Allwood, G. Xiong, C. C. Faulkner, D. Atkinson, D. Petit, and R. P. Cowburn, Magnetic domain-wall logic. *science*, *309*(5741), pp.1688-1692 (2005).
4. Omari, and T. J. Hayward, Chirality-based vortex domain-wall logic gates. *Physical Review Applied*, *2*(4), p.044001 (2014).
5. Lu, and X. R. Wang, Motion of transverse domain walls in thin magnetic nanostripes under transverse magnetic fields. *Journal of Applied Physics*, *107*(8) (2010).
6. Boulle, G. Malinowski, and M. Kläui, Current-induced domain wall motion in nanoscale ferromagnetic elements. *Materials Science and Engineering: R: Reports*, *72*(9), pp.159-187 (2011).
7. Yu, S. Shi, R. Peng, R. Guo, Y. Qiu, G. Wu, Y. Li, M. Zhu, and H. Zhou, Strain-driven magnetic domain wall dynamics controlled by voltage in multiferroic heterostructures. *Journal of Magnetism and Magnetic Materials*, *552*, p.169229 (2022).
8. Donges, N. Grimm, F. Jakobs, S. Selzer, U. Ritzmann, U. Atxitia, and U. Nowak, Unveiling domain wall dynamics of ferrimagnets in thermal magnon currents: Competition of angular momentum transfer and entropic torque. *Physical Review Research*, *2*(1), p.013293 (2020).
9. Berger, Low-field magnetoresistance and domain drag in ferromagnets. *Journal of Applied Physics*, *49*(3), pp.2156-2161 (1978).
10. Berger, Exchange interaction between ferromagnetic domain wall and electric current in very thin metallic films. *Journal of Applied Physics*, *55*(6), pp.1954-1956 (1984).
11. Kläui, H. Ehrke, U. Rüdiger, T. Kasama, R. E. Dunin-Borkowski, D. Backes, L.J. Heyderman, C.A. Vaz, J.A.C. Bland, G. Faini, and E. Cambril, Direct observation of domain-wall pinning at nanoscale constrictions. *Applied Physics Letters*, *87*(10) (2005).
12. L.K. Bogart, D. Atkinson, K. O'Shea, D. McGrouther, and S. McVitie, Dependence of domain wall pinning potential landscapes on domain wall chirality and pinning site

geometry in planar nanowires. *Physical Review B—Condensed Matter and Materials Physics*, *79*(5), p.054414 (2009).

13. Sander, R. Skomski, C. Schmidthals, A. Enders, and J. Kirschner, 1996. Film stress and domain wall pinning in sesquilayer iron films on W (110). *Physical review letters*, *77*(12), p.2566.
14. Barman, A. Ganguly, and A. Barman, March. Configuration and polarization dependent transverse domain wall motion and domain wall switching in ferromagnetic nanowire. In *Spin* (Vol. 3, No. 01, p. 1350001). World Scientific Publishing Company (2013).
15. Yuan, H.Y. and X. R. Wang, Domain wall pinning in notched nanowires. *Physical Review B*, *89*(5), p.054423 (2014).
16. Hwang, I.S., C. K. Fang, and S. H. Chang, Effects of boundaries and point defects on energetics and dynamics of domain walls. *Physical Review B—Condensed Matter and Materials Physics*, *83*(13), p.134119 (2011).
17. Cayssol, F., Ravelosona, D., C. Chappert, J. Ferré, and J.P. Jamet, Domain wall creep in magnetic wires. *Physical review letters*, *92*(10), p.107202 (2004).
18. Goolaup, M. Ramu, C. Murapaka, and W.S. Lew, Transverse domain wall profile for spin logic applications. *Scientific reports*, *5*(1), p.9603 (2015).
19. Wiele, L. Laurson, and G. Durin, Effect of disorder on transverse domain wall dynamics in magnetic nanostrips. *Physical Review B—Condensed Matter and Materials Physics*, *86*(14), p.144415 (2012).
20. Donahue, D. G. Porter, OOMMF User's Guide Version 1.0, Interagency Report NISTIR 6376, [Online], National Institute of Standard and Technology, Gaithersburg, MD, http://math.nist.gov/oommf (1999).
21. Thiaville, Y. Nakatani, J. Miltat, and Y. Suzuki, Micromagnetic understanding of current-driven domain wall motion in patterned nanowires. *Europhysics Letters*, *69*(6), p.990 (2005).
22. Sen, and S. Barman, Optimization of Spin-Polarized Current Induced Domain Wall Velocity in a Magnetic Nano Stripe Using Sinc Pulse—A Computational Study. *Physics of the Solid State*, *66*(8), pp.235-244 (2024).
23. Miron, T. Moore, H. Szambolics, L.D. Buda-Prejbeanu, S. Auffret, B. Rodmacq, S. Pizzini, J. Vogel, M. Bonfim, A. Schuhl, and G. Gaudin,. Fast current-induced domain-wall motion controlled by the Rashba effect. Nature materials, 10(6), pp.419-423 (2011).

24. Hayashi, L. Thomas, C. Rettner, R. Moriya, Y.B. Bazaliy, and S.S. Parkin, Current driven domain wall velocities exceeding the spin angular momentum transfer rate in permalloy nanowires. Physical review letters, 98(3), p.037204 (2007).